

Biophotonics Congress: Biomedical Optics Congress 2018  
(Microscopy/Translational/Brain/OTS) © OSA 2018

# Advances in Single-Photon Detection and Timing for Time Domain Multi-Wavelength Optical Mammography

Edoardo Ferocino<sup>1\*</sup>, Edoardo Martinenghi<sup>1</sup>, Alberto Dalla Mora<sup>1</sup>, Antonio Pifferi<sup>1,2</sup>, Rinaldo Cubeddu<sup>1</sup>, Paola Taroni<sup>1,2</sup>

<sup>1</sup>Politecnico di Milano, Dipartimento di Fisica, Piazza Leonardo da Vinci, 32, 20133, Milan, Italy

<sup>2</sup>Consiglio Nazionale delle Ricerche, Istituto di Fotonica e Nanotecnologie, Politecnico di Milano, Piazza Leonardo da Vinci, 32, 20133, Milan, Italy

Email: edoardo.ferocino@polimi.it

**Abstract:** To enhance photon harvesting and improve data quality, an 8-channel compact SiPM probe and TDC acquisition replace PMTs and TCSPC boards in a time-resolved optical mammograph still providing similar performances for optical properties estimation. © 2018 The Author(s)

**OCIS codes:** (170.6510) Spectroscopy, tissue diagnostics; (170.3830) Mammography; (170.6920) Time-resolved imaging; (170.5280) Photon migration

## 1. Introduction

According to the American Cancer Society, breast cancer is the most common cancer in women, covering nearly 30% of all cancer cases with a 14% death rate [1]. Early diagnosis can significantly improve the survival rate. X-ray imaging is the first technique used in cancer diagnosis, but it suffers from low sensitivity (75%) that may decrease to 50% for radiographic dense breast tissue, and uses ionizing radiation that cannot be considered fully safe. Thus, it is crucial to look for highly sensitive and specific techniques for early cancer detection.

Optical Mammography (OM) is being studied as a complementary technique to X-rays. It uses harmless laser light in the red and Near-Infrared (NIR) region to retrieve the optical properties of tissue, assessing breast tissue composition and investigating correlations with the presence and nature of breast lesions. OM has already led to interesting results not only in cancer detection, but also in risk assessment and monitoring of pathologic outcome of neo-adjuvant chemotherapy [2].

In the past years, our group has developed an instrument for Time-Resolved (TR) multi-wavelength OM. The compressed breast was scanned and illuminated by 7 time-multiplexed pulsed lasers in the visible (VIS: 635, 680, and 785 nm) and in the NIR range (905, 930, 975, and 1060 nm). The transmitted light was collected by a bifurcated fiber bundle with distal ends connected to two photomultiplier tubes (PMTs) for photon detection in the VIS and NIR respectively, while photon timing was achieved by two PC-hosted boards for Time-Correlated Single-Photon Counting (TCSPC) [3]. The main drawbacks we faced during clinical trials on around 200 patients were related to reduced signal level at the longest wavelength (1060 nm), especially for thick dense breasts, leading to low Signal-to-Noise Ratio (SNR) and thus negatively affecting data analysis. Also, the low damage threshold of the NIR PMT forced us to reduce the scanned area not to acquire data close to the boundary of the compressed breast, where the tissue thickness is reduced and would lead to excess light illumination.

To improve the overall data robustness and SNR, especially at 1060 nm, and increase the actual scanned area we present a complete detection chain based on recent advances in the solid-state detectors field along with a cheaper alternative to TCSPC boards to reconstruct the Distribution of Times of Flight (DTOF) curve. The performances were assessed applying two phantom-based protocols: the BIP protocol [4] and MEDPHOT protocol [5].

## 2. System Layout

The new detection chain is made by an 8-channel probe based on Silicon Photomultipliers (SiPMs) and by a multichannel Time-to-Digital Converter (TDC) for the DTOF curve acquisition.

SiPMs are single-photon detectors formed by a matrix of hundreds to thousands of cells, each one hosting a Single-Photon Avalanche Diode (SPAD) and a resistor for passive avalanche quenching and recovery. The cells are packed with high fill factor and connected in parallel, thus sharing a single anode and a single cathode. In recent years, these detectors have been efficiently employed in Time Domain Diffuse Optics (DO) applications [6] thanks to their wide spectral coverage (350-1100 nm) and high quantum efficiency. At the same time, optical fibers and collecting optics can be avoided, thus making possible to use the detector directly in contact with the sample, exploiting the detector's high numerical aperture and increasing light harvesting. Finally, SiPMs represent a compact and cheap alternative to PMTs thanks to their simple read-out electronics that can be easily integrated onto the same probe as the detector. Based on these considerations, our group has developed a multi-channel SiPM probe made of 8 devices (1.3 x 1.3 mm<sup>2</sup> active area, 74% geometrical fill factor, model S13360-1350CS by Hamamatsu Photonics, Japan) mounted in a

squared pattern on a  $1.5 \times 1.5 \text{ cm}^2$  Printed Circuit Board (PCB). The probe replaces the two PMTs and the collecting fiber bundle, and is put at close distance from the compression plate. A commercial 8-channel TDC (SC-TDC-1000/08 S, Surface Concept, Germany) replaces the two TCSPC boards for the acquisition of DTOF curves. It offers higher data throughput than the single TCSPC board (up to 40 Million counts per second, Mcps, vs 10 Mcps with 50% count loss for the board) at a lower cost per channel (<1 k€/channel for the TDC vs ~8 k€/channel for the board). Fig. 1 shows the system layout of the renewed instrument and a close-up of the 8-SiPM detector mounted on the PCB.

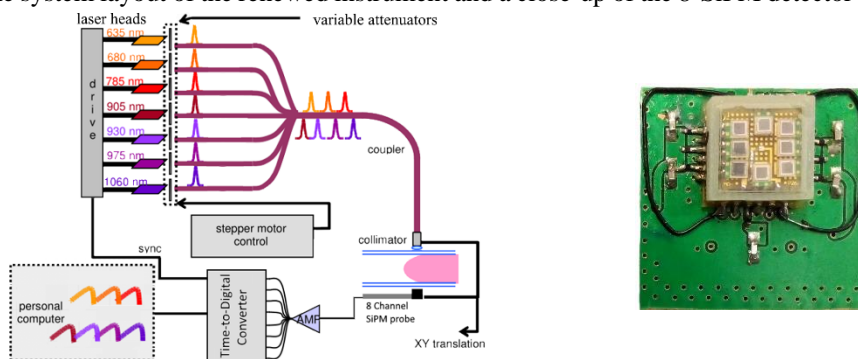


Fig. 1 Left: Renewed system layout: 7 pulsed lasers sequentially illuminate the compressed breast; transmitted light is detected by the 8-channel SiPM probe and the TDC acquires the DTOF curve. Right: detail of the 8 SiPMs mounted onto the  $1.5 \times 1.5 \text{ cm}^2$  PCB.

### 3. BIP protocol: Optical Responsivity

The BIP protocol assesses the basic hardware performances of a TR DO instrument. It was applied to evaluate the overall photon detection efficiency, that is the optical responsivity. A comparison of the measured responsivity of the new and old detection chain is reported in Table 1.

Table 1: Responsivity in  $\text{m}^2\text{sr}$  units for the two systems

Wavelength (nm)	635	680	785	905	933	980	1060
<b>Old Detection Chain</b>	1.85e-08	2.37e-08	6.87e-10	4.63e-09	5.62e-09	1.22e-09	1.08e-11
<b>New Detection Chain</b>	3.70e-06	3.70e-06	2.19e-06	6.02e-07	3.98e-07	2.32e-07	3.31e-08

The use of 8 SiPMs enables an increase in responsivity from a minimum of 1 order of magnitude (at 933 nm) up to 3 orders of magnitude (at 1060 nm). The reasons for this improvement can be found in the higher quantum efficiency of the SiPMs (>25% at 600 nm) with respect to PMTs, along with the elimination of the collecting fiber bundle and related light coupling losses. At the same time, the direct contact of the probe with the compression unit exploits the higher numerical aperture of the SiPM ( $\text{NA} = 0.80$ ) as compared with the fiber bundle ( $\text{NA} = 0.37$ ). Finally, the TDC contributes to increase the overall signal level thanks to its reduced dead time (5.5 ns), thus limiting the count losses when compared to the TCSPC board (~125 ns dead time).

### 4. BIP protocol: Differential Non-Linearity

As part of the BIP protocol we assessed the Differential Non-Linearity (DNL) of the timing electronics. The nominal time width of the TDC time bin, *i.e.* the Least Significant Bit (LSB), is 82 ps. However, we assessed a strong DNL of the time scale up to 0.8 LSB peak-to-peak, thus leading to actual time bin widths between 30 ps and 115 ps. The DNL strongly affects the DTOF curve preventing a good estimation of the optical properties. We tested different DNL correction algorithms and the implemented one reduces the DNL to 0.08 LSB, significantly improving the shape of the DTOF curve. In these conditions, the maximum temporal jitter is around 150 ps, higher than for the TCSPC board (~7 ps), but still acceptable for our application, as confirmed by the performances reported in the following.

### 5. MEDPHOT protocol: Linearity and accuracy

The MEDPHOT protocol assesses the performances of the detection chain based on the accuracy and linearity of the reconstructed optical properties of 32 solid phantoms covering a wide range of absorption and reduced scattering values ( $\mu_a$  ranging from  $0 \text{ cm}^{-1}$  to  $0.35 \text{ cm}^{-1}$  in steps of  $0.05 \text{ cm}^{-1}$ , labeled with numbers, and  $\mu_s'$  = 5, 10, 15, 20  $\text{cm}^{-1}$  labeled with letters) mimicking the properties of tissues. As an example, Fig. 2 displays the linearity performance for the absorption and reduced scattering coefficient by plotting respectively the measured  $\mu_a$  and  $\mu_s'$  values against the nominal ones at 785 nm. The results show good linearity of the system up to  $\mu_a = 0.3 \text{ cm}^{-1}$ . Linearity on  $\mu_s'$  is good

up to  $10 \text{ cm}^{-1}$  after which a maximum integral non-linearity of 21% arises. Linearity is preserved regardless the  $\mu_a$  value except for the most absorbing phantom (number 8,  $\mu_a = 0.35 \text{ cm}^{-1}$ ).

The accuracy is evaluated as the percentage error of the reconstructed optical parameters with respect to nominal values: the median of errors is 12% on  $\mu_a$  and 21% on  $\mu_s'$ . These errors are comparable with those of the previous system.

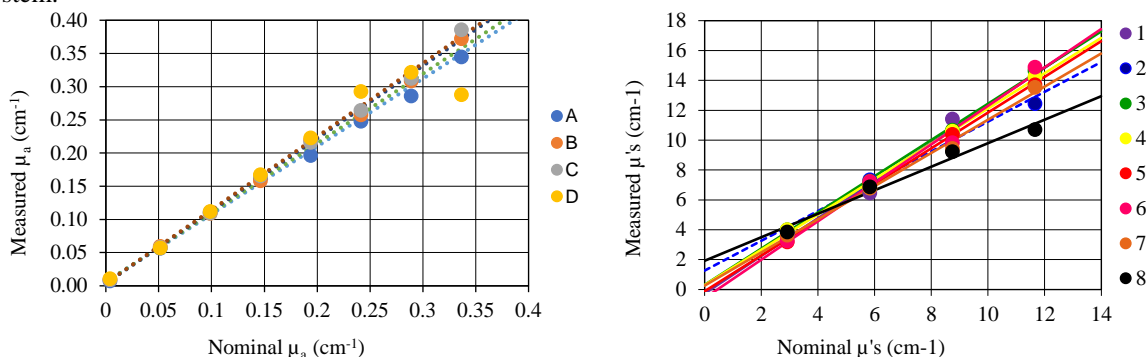


Fig. 2 Linearity performance on  $\mu_a$  (left) and  $\mu_s'$  (right) at 785 nm.

## 6. Scan procedure

In the old instrument, the high sensibility of PMTs to excessive light exposure forced us to make a pre-scan of the compressed breast to get the actual size of the area that could be scanned without damaging the detectors. This represented a wasting time procedure. Furthermore, the area scanned with the NIR detector was smaller than the one scanned with the VIS detector. On the contrary, the SiPMs are insensitive to heavy light exposure at any wavelengths. Thus, we could remove the pre-scan and improve the scanning procedure to include the full compressed breast.

## 7. Conclusions

We propose a complete detection chain formed by an 8-channel SiPM probe and a multi-channel TDC for our optical mammograph, so to increase the overall signal level and data robustness, especially at the longest (1060 nm) wavelength. The new detection chain increases the optical responsivity of up to a factor of 1000, while keeping comparable performances in the optical properties estimation as compared with the previous system. Furthermore, the new detection chain is a more robust and cheaper alternative to the more conventional detection chain for TD DO applications formed by PMTs and TCSPC boards. These results led us to plan preliminary sessions of *in vivo* measures to assess the instrument performances in real operational conditions in view of a potential use for neoadjuvant chemotherapy monitoring and prediction of pathologic outcome.

## 8. Acknowledgement

The research leading to these results has received partial funding from the European Union's Horizon 2020 research and innovation program under grant agreement No 731877. SOLUS ([www.solus-project.eu](http://www.solus-project.eu)) is an initiative of the Photonics Public Private Partnership. The authors declare that there are no conflicts of interest related to this article.

## 9. References

- [1] R. L. Siegel, K. D. Miller, and A. Jemal, "Cancer statistics," *CA Cancer J Clin* **66**, 7–30 (2016).
- [2] D. Grosenick, K. T. Moesta, M. Möller, J. Mücke, H. Wabnitz, B. Gebauer, C. Stroszczyński, B. Wassermann, P. M. Schlag, and H. Rinneberg, "Time-domain scanning optical mammography: I. Recording and assessment of mammograms of 154 patients," *Phys. Med. Biol.* **50**, 2429–2449 (2005).
- [3] P. Taroni, A. Pifferi, E. Salvagnini, L. Spinelli, A. Torricelli, and R. Cubeddu, "Seven-wavelength time-resolved optical mammography extending beyond 1000 nm for breast collagen quantification.," *Opt. Express* **17**, 15932–46 (2009).
- [4] H. Wabnitz, D. R. Taubert, M. Mazurenka, O. Steinkellner, A. Jelzow, R. Macdonald, D. Milej, P. Sawosz, M. Kacprzak, A. Liebert, R. Cooper, J. Hebden, A. Pifferi, A. Farina, I. Bargigia, D. Contini, M. Caffini, L. Zucchelli, L. Spinelli, R. Cubeddu, and A. Torricelli, "Performance assessment of time-domain optical brain imagers, part 1: basic instrumental performance protocol," *J. Biomed. Opt.* **19**, 86010 (2014).
- [5] A. Pifferi, A. Torricelli, A. Bassi, P. Taroni, R. Cubeddu, H. Wabnitz, D. Grosenick, M. Möller, R. Macdonald, J. Swartling, T. Svensson, S. Andersson-Engels, R. L. P. van Veen, H. J. C. M. Sterenborg, J.-M. Tualle, H. L. Nghiem, S. Avrillier, M. Whelan, and H. Stamm, "Performance assessment of photon migration instruments: the MEDPHOT protocol.," *Appl. Opt.* **44**, 2104–2114 (2005).
- [6] A. Dalla Mora, D. Contini, S. Arridge, F. Martelli, A. Tosi, G. Boso, A. Farina, T. Durduran, E. Martinenghi, A. Torricelli, and A. Pifferi, "Towards next-generation time-domain diffuse optics for extreme depth penetration and sensitivity," *Biomed. Opt. Express* **6**, 1749–1760 (2015).